Journal of Mechanical Science and Technology (KSME Int. J.), Vol. 20, No. 10, pp. 1557~1566, 2006 **1557**

Optimization Analysis of Trajectory for Re-Entry Vehicle Using Global Orthogonal Polynomial

Daewoo Lee*

Department of Aerospace Engineering, Pusan National University, Jangjun-Dong, Kumjung-Ku, Pusan 609-735, Korea

We present a procedure for the application of global orthogonal polynomial into an atmospheric re-entry maneuvering problem. This trajectory optimization is imbedded in a family of canonically parameterized optimal control problem. The optimal control problem is transcribed to nonlinear programming via global orthogonal polynomial and is solved a sparse nonlinear optimization algorithm. We analyze the optimal trajectories with respect to the performance of re-entry maneuver.

Key Words : Re-Entry Vehicle, Trajectory Optimization, Bank Angle, Angle of Attack, Global Orthogonal Polynomial, Heating Rate Constraint

1. Introduction

Future as well as present space projects, such as laboratories stationed in orbit, will only be attractive if transportation can be provided at low operational cost. Economic alternatives to the manned Space Shuttle are the development of the reusable payload lunch vehicle. Their feasibilities have been currently being investigated in the United States, EU. Although the Hope-X of Japan is not a reusable launch vehicle, it is developing as the first re-entry vehicle of Japan. A key issue is, if safe and accurate flight profile from a lunch to atmospheric re-entry and landing can be achieved despite the vehicle's several constraints, to avoid an expensive recovery and long turnaround periods. Furthermore, the hot issue of atmospheric re-entry is to deliver the re-entry vehicle to a desired destination with an energy state sufficient for approach and landing. For achieving this propose, adequate reference trajectory and guidance law are necessary. Typically, on-board guidance systems use a nominal reference trajectory to predict the flight range and trajectory control to keep the prediction within satisfactory permissible error bounds. In case of a predicted flight range miss, the reference trajectory is modified (Lee and Cho, 2000).

The problem of trajectory optimization (Betts, 1998) for re-entry vehicle maneuvering has been not a few addressed in the literature. Baker et al. used the Calculus Of Variation (COV) algorithms to find optimal re-entry trajectory in 1971. B. P. and Sng used the quasilinearization to get the numerical solution of the constrained re-entry vehicle trajectory in 1980. Lu in 1997 and Lee and Cho in 2002 and 2004, presents the reference trajectory by a sequential quadratic programming.

In a variety of trajectory optimization problem, direct methods have been used extensively. In their traditional collocation schemes such as Gauss-Lobatto quadrature rules and Simpson's rules, the state equations are approximated by numerically integrating the state equations over the subinterval, therefore the state constraints are not imposed exactly at each nodes. The choice of global orthogonal polynomial (Han et al., 1989 ; Fahroo and Ross, 1998) for collocation optimal trajectory problem is recently used to overcome this disadvan-

* **E-mail** : baenggi@pusan.ac.kr
TEL : +82-51-510-2329; **FAX** : +82-51-513-3760
Department of Aerospace Engineering, Pusan National University, Jangjun-Dong, Kumjung-Ku, Pusan 609-735, Korea. (Manuscript **Received** November 18, 2005; **Revised** July 21, 2006)

tage.

In this paper, we show the optimal reference trajectories for re-entry vehicle maneuvering using global orthogonal polynomial. These trajectories are shown in both the case of "without heating rate constraint" and "with heating rate constraint". The control parameters used are bank angle for long period control and angle of attack for short period control. We analyze the performance of trajectories with respect to the maneuver of the re-entry vehicle.

2. Maneuvering Re-Entry Vehicle Problem

2.1 Description of the re-entry dynamics

This idea is demonstrated by arbitrarily choosing a particular set of coordinates that describe the state of the vehicle by the six-dimensional vector, $\bar{x}=(R, V, \gamma, \phi, \theta, \psi)$ consisting of its radial position, Earth relative speed, flight path angle, latitude, longitude, heading angle respectively. The equations of re-entry motion (Regan, 1993) for space vehicles can be described under the following assumptions.

(1) The earth is assumed to be a rotating sphere.
(2) The non-thrusting re-entry vehicle is assumed to be a point mass from the vertical plane of the earth.

With these assumptions, the dynamics of re-entry (Vinh et al., 1980) are

$$\dot{R}=V\sin\gamma$$

$$\dot{V}=-D-\frac{\mu\sin\gamma}{R^2}+\Omega_E^2 R\cos\phi(\sin\gamma\cos\phi-\cos\gamma\sin\phi\sin\psi)$$

$$V\dot{\gamma}=Du+\left(V^2-\frac{\mu}{R}\right)\frac{\cos\gamma}{R}+2\Omega_E V\cos\phi\cos\psi+\Omega_E^2 R\cos\phi(\cos\gamma\cos\phi-\sin\gamma\sin\psi\sin\phi) \quad (1)$$

$$\dot{\phi}=\frac{V\cos\gamma\sin\psi}{R}$$

$$\dot{\theta}=\frac{V\cos\gamma\cos\psi}{R\cos\phi}$$

$$\dot{\psi}=\frac{L\sin\sigma}{V\cos\gamma}-\frac{V\cos\gamma\cos\psi\tan\phi}{R}+2\Omega_E(\tan\gamma\sin\psi\cos\phi-\sin\phi)-\frac{\Omega_E^2 R}{V\cos\gamma}\cos\psi\sin\phi\cos\phi$$

$$D=\frac{\rho S_{ref}V^2C_D}{2m} \quad (2)$$

$$L=\frac{\rho S_{ref}V^2C_L}{2m} \quad (3)$$

where, D is the drag acceleration, L lift acceleration, and μ is the gravity constant. The angular velocity of the rotation of earth is Ω_E. u is the function of the bank angle as the control variable and the vertical component of the lift-to-drag ratio, and the bank angle σ is defined as the angle between the lift vector and $(\bar{R}, \bar{V})$, C_L and C_D are the lift coefficient and drag coefficient, respectively. S_{ref} is the reference surface area, and the mass of space vehicle.

The dynamic pressure (q) is defined as $\rho V^2/2$. The atmospheric density ρ is the exponentially varying.

$$\rho=\rho_0\exp\left(-\frac{R-R_0}{h_s}\right) \quad (4)$$

where ρ_0 is the density at sea level, $h=R-R_0$ is the altitude, and h_s is the density scale-height. The lift and drag coefficients used in this analysis are given as

$$C_L(\alpha)=C_{L_0}+C_{L_\alpha}\alpha$$
$$C_D(\alpha)=C_{D_0}+C_{D_\alpha}\alpha+C_{D_{\alpha 2}} \quad (5)$$

where C_{L_0} and C_{D_0} are the zero-lift coefficient and the zero-drag coefficient respectively. α is the angle of attack.

$$C_{L_0}=-0.207,\ C_{L_\alpha}=1.676,$$
$$C_{D_0}=0.079,\ C_{D_\alpha}=-0.353,\ C_{D_{\alpha 2}}=2.40 \quad (6)$$

2.2 Path constraints

Inequality constraints can be imposed on several parameters during atmospheric re-entry. In this study, we imposed inequality constraint on heating rate, bank angle and angle of attack, which are control inputs.

$$0 \le q \le q_{\max} \tag{7}$$

$$\sigma_{\min} \le \sigma \le \sigma_{\max} \tag{8}$$

$$\alpha_{\min} \le \alpha \le \alpha_{\max} \tag{9}$$

The heating rate (Betts, 2001) is serious constraint in high altitude region, and is decided by the performance of the protective heat tiles. It is function of R, V, and α, and is given by

$$q(R, V, \alpha) = q_\alpha(\alpha)\, q_r(R, V) \tag{10}$$

$$\begin{aligned} q_\alpha &= a_1 + a_2\alpha + a_3\alpha^2 + a_4\alpha^3 \\ q_r &= b_1 \rho^{b_2} V^{b_3} \end{aligned} \tag{11}$$

where, a_i $(i=1,2,3,4)$ and b_j $(j=1,2,3)$ are constants.

2.3 Performance index

In general, the performance index for re-entry problem is chosen by the objective of mission. For examples, total heating accumulated in the airframe (Lee and Cho, 2002) is minimized to minimize heating, the inclination of drag acceleration is minimized to impose physical characteristic of re-entry flight, and the amount of control margin is maximized to correct for unpredictable flight conditions, and so on.

In this study, we choose the final latitude as the performance index to maximize the cross-range for an equatorial orbit.

$$\min J = \min \phi(t_f) \tag{12}$$

2.4 Boundary conditions

In this study, the boundary conditions for the maneuver of re-entry vehicle are defined that all the initial conditions are completely specified, while the only R, V, γ in the final conditions are specified. The initial conditions are collected to form a set of navigation parameters and final conditions are target parameters for a TAEM (Terminal Area Energy Management). Therefore, boundary conditions $\phi[x(t_f), t_f] = 0$ are given as

$$\begin{aligned} R(t_0) &= r_0 = 6450.452 \times 10^3 \text{ m} \\ V(t_0) &= V_0 = 7802.88 \text{ m/sec} \\ \gamma(t_0) &= \gamma_0 = -1 \text{ deg} \\ \phi(t_0) &= \phi_0 = 0 \text{ deg} \\ \theta(t_0) &= \theta_0 = 0 \text{ deg} \\ \psi(t_0) &= \psi_0 = 0 \text{ deg} \end{aligned} \tag{13}$$

$$\begin{aligned} R(t_f) &= r_f = 6395.588 \times 10^3 \text{ m} \\ V(t_f) &= V_f = 762 \text{ m/sec} \\ \gamma(t_f) &= \gamma_f = -5 \text{ deg} \\ \phi(t_f) &= \phi_f = \text{Free} \\ \theta(t_f) &= \theta_f = \text{Free} \\ \psi(t_f) &= \psi_f = \text{Free} \end{aligned} \tag{14}$$

The initial time is zero and final time is free.

$$t_0 = 0, \; t_f = \text{Free} \tag{15}$$

2.5 Definition of optimal control Problem

The reference trajectory for the maneuvering re-entry vehicle under consideration in this study is computed by solving the following optimal control problem (Calise and Leung, 1994). Thus this problem is summarized to find the control histories of bank angle and angle of attack on the time interval $t \in [0, t_f]$ that minimize the objective functional of Eq. (12) subject to the differential equations of Eqs. (1) ~ (6), the path constraints of Eqs. (7) ~ (9), and boundary conditions of Eqs. (13) ~ (14).

The bank angle is used for control in long period deviation. On the contrary, to minimize the effect of the bank reversals and other transient effects such as density gradients, a change in angle of attack from the reference trajectory can be commanded to compensate for short period drag trajectory deviations from the reference trajectory.

$$u(t) = [\sigma(t), \; \alpha(t)] \tag{16}$$

The Hamiltonian function is defined as

$$\begin{aligned} H = {} & \lambda_R V \sin\gamma + \lambda_V \left[\frac{\mu \sin\gamma}{R^2} \right. \\ & \left. + \Omega_E^2 R \cos\phi (\sin\gamma \cos\phi - \cos\gamma \sin\phi \sin\psi) \right] \\ & + \lambda_\gamma \left[\frac{Du}{V} + \left(V - \frac{\mu}{RV} \right) \frac{\cos\gamma}{R} + 2\Omega_E \cos\phi \cos\psi \right. \\ & \left. + \Omega_E^2 \frac{R}{V} \cos\phi (\cos\gamma \cos\phi + \sin\gamma \sin\psi \sin\phi) \right] \end{aligned} \tag{17}$$

$$+\lambda_\phi\left[\frac{V\cos\gamma\sin\psi}{R}\right]+\lambda_\theta\left[\frac{V\cos\gamma\cos\psi}{R\cos\phi}\right]$$
$$+\lambda_\psi\left[\frac{L\sin\sigma}{V\cos\gamma}-\frac{V\cos\gamma\cos\psi\tan\phi}{R}\right.$$
$$+2\Omega_E(\tan\gamma\sin\psi\cos\phi-\sin\phi)$$
$$\left.-\frac{\Omega_E^2 R}{V\cos\gamma}\cos\psi\sin\phi\cos\phi\right]$$

When Hamiltonian function is used, the co-state equations are defined as

$$\dot{\lambda}_R=-\lambda_V[2\mu/R^3\sin\gamma$$
$$+\Omega^2\cos\phi(\sin\gamma\cos\phi-\cos\gamma\sin\psi\sin\phi)]$$
$$-\lambda_\gamma[-(V/R^2-2\mu/R^3/V)\cos\gamma$$
$$+\Omega^2/V\cos\phi(\cos\gamma\cos\phi+\sin\gamma\sin\psi\sin\phi)] \quad (18a)$$
$$+\lambda_\phi V\cos\gamma\sin\psi/R^2$$
$$+\lambda_\theta V\cos\gamma\cos\psi R^2/\cos\phi$$
$$-\lambda_\psi[V/R^2\cos\gamma\cos\psi\tan\phi$$
$$-\Omega^2/V/\cos\gamma\cos\psi\sin\phi\cos\phi]$$

$$\dot{\lambda}_V=-\lambda_R\sin\gamma$$
$$-\lambda_\gamma[-L\cos\sigma/V^2+(\mu/R^2/V^2+1/R)\cos\gamma$$
$$-\Omega^2R/V^2\cos\phi(\cos\gamma\cos\phi+\sin\gamma\sin\psi\sin\phi)] \quad (18b)$$
$$-\lambda_\phi\cos\gamma\sin\psi/R-\lambda_\theta\cos\gamma\cos\psi/R/\cos\phi$$
$$-\lambda_\psi[-L\sin\sigma/V^2/\cos\gamma-1/R\cos\gamma\cos\psi\tan\phi$$
$$+\Omega^2R/V^2/\cos\gamma\cos\psi\sin\phi\cos\phi]$$

$$\dot{\lambda}_\gamma=-\lambda_R V\cos\gamma-\lambda_V[-\mu/R^2\cos\gamma$$
$$+\Omega^2R\cos\phi(\cos\gamma\cos\phi+\sin\gamma\sin\psi\sin\phi)]$$
$$-\lambda_\gamma[(\mu/R^2/V-V/R)\sin\gamma$$
$$+\Omega^2R/V\cos\phi(-\sin\gamma\cos\phi+\cos\gamma\sin\psi\sin\phi)]$$
$$+\lambda_\phi V\sin\gamma\sin\psi/R+\lambda_\theta V\sin\gamma\cos\psi/R/\cos\phi \quad (18c)$$
$$-\lambda_\psi[L\sin\sigma/V/\cos^2\gamma\sin\gamma]$$
$$+V/R\sin\gamma\cos\psi\tan\phi$$
$$+2\Omega(1+\tan^2\gamma)\sin\psi\cos\phi$$
$$-\Omega^2R/V/\cos^2\gamma\cos\psi\sin\phi\cos\phi\sin\gamma]$$

$$\dot{\lambda}_\phi=\lambda_V[-\Omega^2R\sin\phi(\sin\gamma\cos\phi-\cos\gamma\sin\psi\sin\phi)$$
$$+\Omega^2R\cos\phi(-\sin\gamma\sin\phi-\cos\gamma\sin\psi\cos\phi)]$$
$$-\lambda_\gamma[-2\Omega\cos\psi\sin\phi$$
$$-\Omega^2R/V\sin\phi(\cos\gamma\cos\phi+\sin\gamma\sin\psi\sin\phi)$$
$$+\Omega^2R/V\cos\phi(-\cos\gamma\sin\phi+\sin\gamma\sin\psi\cos\phi) \quad (18d)$$
$$-\lambda_\theta V\cos\gamma\cos\psi/R/\cos^2\phi\sin\phi$$
$$-\lambda_\psi[-V/R\cos\gamma\cos\psi(1+\tan^2\phi)$$
$$+2\Omega(-\tan\gamma\sin\psi\sin\phi-\cos\phi)$$
$$-\Omega^2R/V/\cos\gamma\cos\psi\cos^2\phi$$
$$+\Omega^2R/V/\cos\gamma\cos\psi\sin^2\phi]$$

$$\dot{\lambda}_\theta=0 \quad (18e)$$

$$\dot{\lambda}_\psi=\lambda_V\Omega^2R\cos\phi\cos\gamma\cos\psi\sin\phi$$
$$-\lambda[-2\Omega\sin\psi\cos\phi$$
$$+\Omega^2R/V\cos\phi\sin\gamma\cos\psi\sin\phi]$$
$$-\lambda_\phi V\cos\gamma\cos\psi/R+\lambda_\phi V\cos\gamma\sin\psi/R/\cos\phi \quad (18f)$$
$$-\lambda_\psi[V/R\cos\gamma\sin\psi\tan\phi]$$
$$+2\Omega\tan\gamma\cos\psi\cos\phi$$
$$+\Omega^2R/V/\cos\gamma\sin\psi\sin\phi\cos\phi$$

and the auxiliary function, $\Phi=\phi=\nu^T\phi$ is

$$\Phi=\phi=\nu_1(R_f-2098.29\times10^4)$$
$$+\nu_2(V_f-2500)+\nu_3\left(\gamma_f+\frac{5\pi}{180}\right) \quad (19)$$

From the transversality conditions, $\lambda(t_f)=[\partial\Phi/\partial x]_{t=t_f}$ we obtain the following co-state terminal conditions for the re-entry trajectory:

$$\lambda_R(t_f)=\nu_1,\ \lambda_V(t_f)=\nu_2,\ \lambda_\gamma(t_f)=\nu_3,$$
$$\lambda_\phi(t_f)=1,\ \lambda_\theta(t_f)=\lambda_\psi(t_f)=0 \quad (20)$$

where ν is the constant Lagrange multiplier. Furthermore, the additional transversality condition for the Hamiltonian function should be satisfied at t_f.

$$\left[\frac{\partial\Phi}{\partial t}+H\right]_{t=t_f}=0 \quad (21)$$

From Eq. (21), we get the following condition as another boundary equation.

$$H(t_f)=0 \quad (22)$$

3. Numerical Implications

Many numerical algorithms to solve optimal control problems have been developed, but they can be grouped into two major categories: indirect and direct methods. Indirect methods are theoretically based on Pontryagin's minimum principle, which characterizes the set of optimal states and controls in terms of the solution of a boundary value problem. One of the indirect methods becomes a second order method and yields solutions of high precision, Hence, it is very sensitive to small change in co-state initial conditions. The indirect methods have the associated difficulties caused by instability of the initial value problem for the system of differential equations and by the requirement for good initial guesses for iterative

solutions of nonlinear problem. Therefore, these methods are not typically used to solve complex problem due to their inherent small radii of convergence and the additional labor required in deriving the optimal conditions.

On the contrary, in recent years, direct methods have been used extensively in a variety of trajectory optimization problems (Betts, 1998; Hull, 1997). Direct methods are based on discretizing the control and/or state variable time history at the nodes of discretization, and transforming the optimal control problem to a nonlinear programming (NLP) problem and then solving the resulting nonlinear programming problem. Their advantage over indirect methods is their wider radius of convergence to an optimal solution. In addition, since the necessary conditions do not have to be derived, the direct methods can be quickly used to solve a number of practical trajectory optimization problems.

For better numerical conditioning of the trajectory optimization process, R is normalized by the Earth radius, R_E. V is normalized by $\sqrt{g_0 R_E}$, D and L are normalized by g_0, and Ω_E is normalized by $\sqrt{R_E g_0}$.

In this paper, a numerical optimization solver, SNOPT is used to solve an optimization for re-entry vehicle maneuvering. For the re-entry problem, there are 12 differential equations describing the states [Eq. (1)], and co-states [Eq. (18)], and 13 unknowns $[\lambda_R(t_0), \lambda_V(t_0), \lambda_\gamma(t_0), \lambda_\phi(t_0), \lambda_\theta(t_0), \lambda_\psi(t_0), \nu_1, \nu_2, \nu_3, \phi(t_f), \theta(t_f), \psi(t_f), t_f]$ and 13 boundary conditions [Eq. (13), $R(t_f), V(t_f), \gamma(t_f), \lambda_\phi(t_f), \lambda_\theta(t_f), \lambda_\psi(t_f)$, Eq. (22)].

To formulate this re-entry problem, the numerical techniques in Ref. Bryson are adopted and modified. The unknown parameters [ν, t_f, unknown initial co-states] are guessed initially, and the state and co-state equations are integrated to final time by implicating the controls. Corrections to the guessed values and missing initial conditions are assumed to be satisfied if the terminal condition norm is less than 10^{-7}. A trial-and-error strategy is used until good initial co-state values are obtained.

4. Collocation Using Global Orthogonal Polynomial

The time histories of states or controls can be obtained by using an interpolation. In most collection schemes, linear or cubic splines are used as the interpolating polynomials. At present, instead of using piecewise-continuous polynomials as the interpolant between sub-interval, global orthogonal polynomials such as Legendre and Chebyshev polynomial (Lee, 2003) can be used widely. These are used originally in spectral methods for solving fluid dynamics problem, but their use in solving optimal control problem has created a new way of transforming them to NLP problem, because they have close relationship which can be used to derive simple rules for transforming the original optimal control problem to algebraic equations. We use the Legendre polynomial in this paper.

The basic idea of this method is to seek approximations for the state, co-state and control functions in terms of their values at some carefully chosen node points which are called Legendre-Gauss-Lobatto (LGL). LGL points have a merit of small error with respect to the least square method. These have fixed end points at -1 and 1.

$$t \in [t_o, t_f] = [-1, 1] : \tau = \frac{(\tau_f - \tau_0)\, t + (\tau_f - \tau_0)}{2} \quad (23)$$

This method is developed by Elnagar, Fahroo and Ross, and has an objective to transcribe the continuous time optimal control problem into a nonlinear programming problem. It is beyond the scope of this paper to provide a detailed description of the Pseudospectral Legendre. A conclusive summary of this method is briefly provided here in order to maintain continuity.

Let L_N be the Legendre polynomial of degree on the interval $[-1, -1]$. In the Legendre collocation approximation of the state and co-state equations, we use the LGL points, t_l, $l=0, 1, 2, \cdots, N$ which are given by $t_0 = -1, t_f = 1$. For $1 \leq l \leq N-1$, t_l are the zeros of $\dot{L}_N$, the derivative of the Legendre polynomial L_N. The continuous states, co-states, and control variables by N-order

Legendre polynomial are,

$$x^N(t)=\sum_{l=0}^{N}x(t_l)\,\phi_l(t)$$
$$u^N(t)=\sum_{l=0}^{N}u(t_l)\,\phi_l(t) \tag{24}$$
$$\lambda^N(t)=\sum_{l=0}^{N}\lambda(t_l)\,\phi_l(t)$$

Since the $\phi_l(t)$ satisfies the characteristic of the Kronecker delta

$$x^N(t_l)=x(t_l)=a_k$$
$$u^N(t_l)=u(t_l)=b_k \tag{25}$$
$$\lambda^N(t_l)=\lambda(t_l)=a_k$$

To express the time derivative of the state and co-state in terms of the state and co-state at the collocation points respectively, we differentiate the state and co-state in Eq. (24) which results in a matrix multiplication of the following forms:

$$\dot{x}^N(t_k)=\sum_{l=0}^{N}\dot{\phi}_l(t_k)\,x(t_l)=\sum_{l=0}^{N}D_{kl}x(t_l)=d_k$$
$$\dot{\lambda}^N(t_k)=\sum_{l=0}^{N}\dot{\phi}_l(t_k)\,\lambda(t_l)=\sum_{l=0}^{N}D_{kl}\lambda(t_l)=e_k \tag{26}$$

where D_{kl} is the differentiation matrix with size of $(N+1)\times(N+1)$.

Minimize the performance index:

$$J^N(x,u)=M(x_N,\tau_f)+\frac{\tau_f-\tau_0}{2}\sum_{k=0}^{N}L(x_k,u_k)\,w_k \tag{27}$$

subject to the state equations, boundary conditions, and inequality constraints. w_k is the weight.

$$\frac{\tau_f-\tau_0}{2}f(x_k,u_k)-d_k=0 \tag{28}$$

$$\phi[a_0,\tau_0]=0,\ \phi[a_N,\tau_f]=0 \tag{29}$$

$$g(a_k,b_k)\le 0 \tag{30}$$

where, node number $k=0,1,2,3,\cdots,N$

5. Results of the Re-Entry Vehicle Maneuver

We start optimization by guess of the unknown parameters. The physical parameters used in this paper are shown in Table 1.

Table 1 Physical parameters

Parameter	Value
S_{ref}	250 m^2
ρ_0	1.225 kg/m^3
R_E	6.3713×10^6 m
h_s	7254.24 m
q_{max}	794.986 KW/m^2
Ω_E	7.292e-5 rad/s
μ	3.9822×10^{14} m^3/s^2
m	102279 kg
σ_{min}	$-\pi$
σ_{max}	π
α_{min}	0
α_{max}	π

The results in Figs. 1~10 are shown in both the case of "Without heating rate constraint" and "With heating rate constraint". Final time of the former is 2370 sec, the latter is 2590 sec. It is seen from Fig. 1 that the altitude without heating rate constraint has actual oscillation maneuvers of three or four times as compared with the altitude with heating rate constraint during atmospheric re-entry. These maneuvers enable the re-entry vehicle to fly in a high density region in the same times due to no heating rate constraint. During the serial fall in altitude, Earth-relative speed in Fig. 2 is reduced so that the vehicle can arrive at the TAEM (Terminal Area Energy Management) interface with the prescribed final speed of 2500 ft/s. Fig. 3 represents the time histories of the flight path angle. Figs. 4 and 5 give geometric informations for the optimal trajectories. Moreover, as alluded to earlier, the latitudes in Fig. 4 are considered as the performance index. The latitude of -37 degree in the case of "Without heating rate constraint" is smaller than the latitude of -34.64 degree in the other case. The difference of 2.36 degree is due to an atmospheric density of application of heating rate constraint. In Fig. 6, the optimal heading angle is represented.

The next key feature of the results is the time histories of bank and angle of attack which are shown in Figs. 7 and 8. It can be seen that, the initial bank angle of the case without heating rate

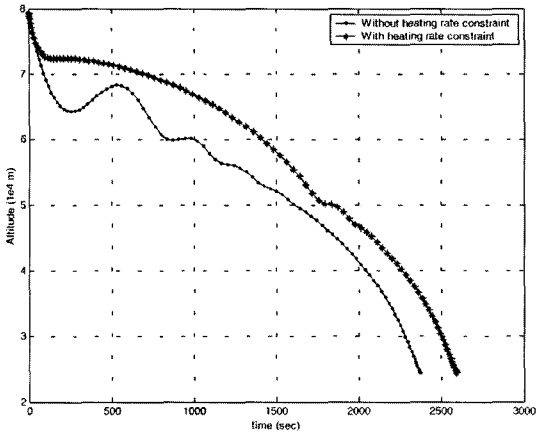

Fig. 1 Altitudes vs time

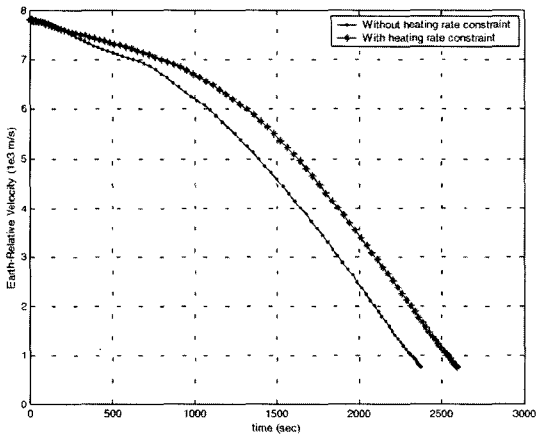

Fig. 2 Earth-relative speeds vs time

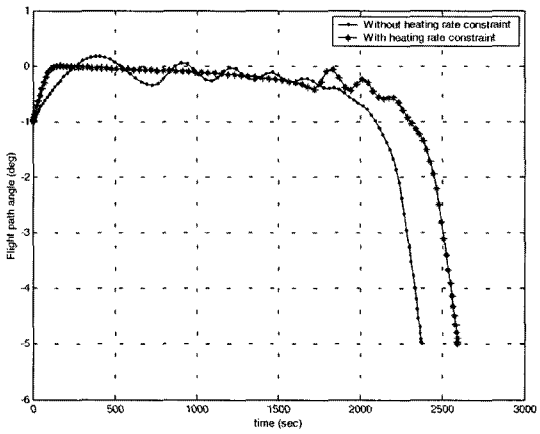

Fig. 3 Flight path angles vs time

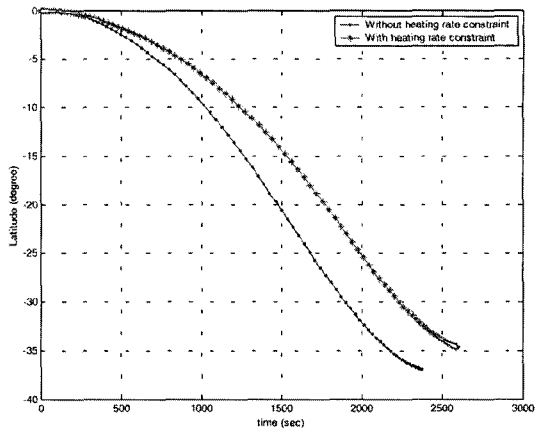

Fig. 4 Latitudes vs time

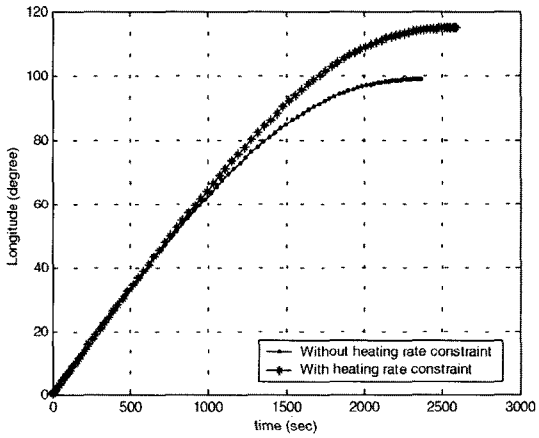

Fig. 5 Longitude vs time

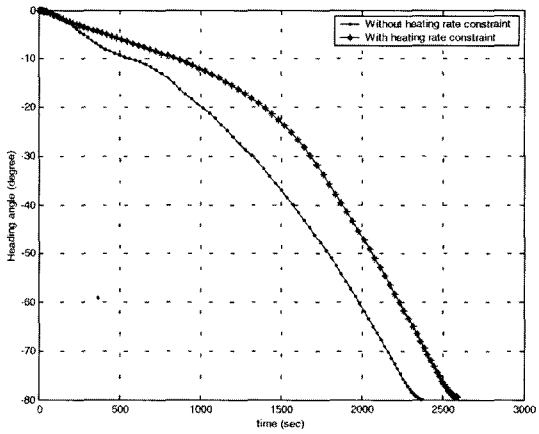

Fig. 6 Heading angles vs time

constraint is 115 degree which larger then the case with heating rate constraint, because altitude does not decrease monotonically but actually has sudden drops in altitude. The reason that the

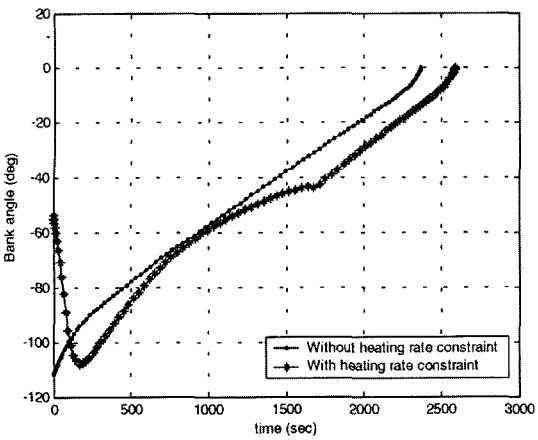

Fig. 7 Bank angles vs time

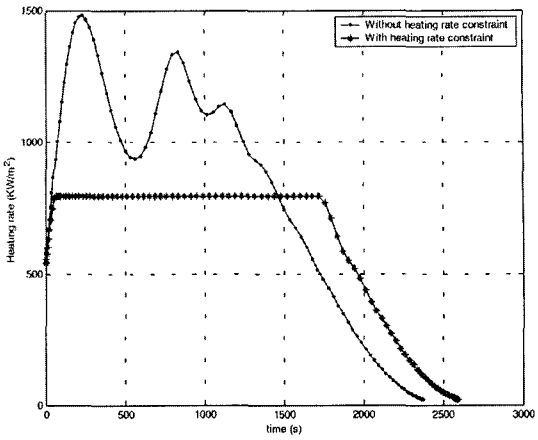

Fig. 9 Heating rates vs time

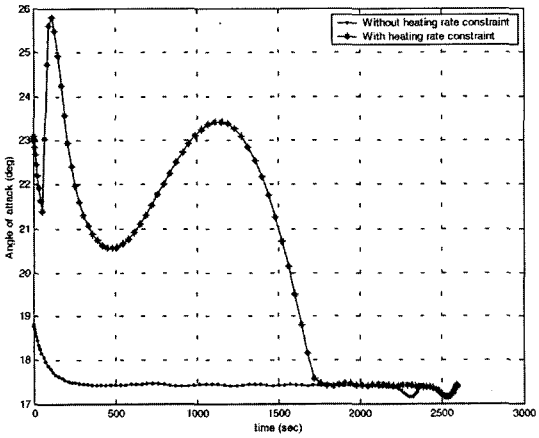

Fig. 8 Angle of attacks vs time

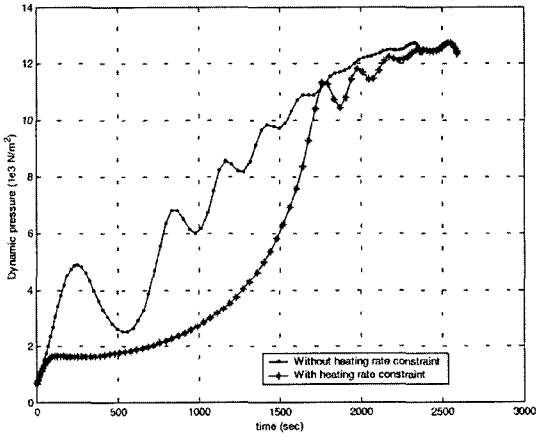

Fig. 10 Dynamic pressures vs time

altitude has several drop maneuvers is because the short period of flying time can make the minimization of latitude. On the contrary, in the case with heating rate constraint, the angle of attack increases twice so dramatically before approaching to the final time. This reason is because the re-entry vehicle needs to deplete speed before arriving at the final position in order to satisfy the condition at TAEM interface. The bank·angle is bounded within a range of 115 degree and the angle of attack 9 degree due to the characteristic of period.

Fig. 9 shows the time histories of heating rate. In the case with heating rate constraint, we can verify the sudden change of the bank angle and angle of attack near 1700 sec as well as the heating rate. Fig. 10 gives that a low density should be sustained until 1700 sec in the case with heating rate constraint.

Fig. 11 shows the time history of Hamiltonian. Since for re-entry problem the Hamiltonian is not an explicit function of time and terminal time is free, the Hamiltonian along an optimal trajectory must be zero. The result obtained from the case without heating rate gives strong evidence that trajectories obtained the optimization using global orthogonal polynomial are close to an optimal trajectories. On the contrary, the case with heating rate brings forth a little optimal error. However, it is permissible with respect to scale.

Fig. 12 shows both the dynamic pressure and the altitude of the case without heating rate constraint. From this figure, we know that several local maxima in altitude occur at point where the

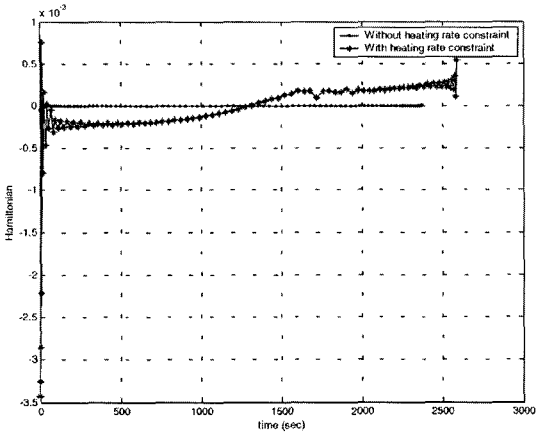

Fig. 11 Hamiltonians vs time

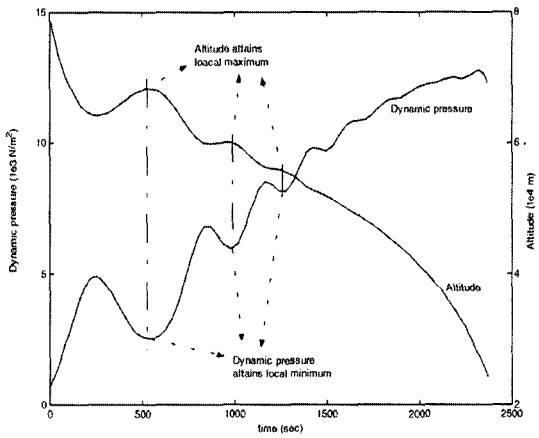

Fig. 12 Dynamic pressure and altitude vs time

dynamic pressure is also local minima because densities in these points are local minima.

6. Conclusions

The performance analyses of optimal trajectories for re-entry maneuver via global orthogonal polynomial are presented. The results are divided as both the case of "without heating rate constraint" and "with heating rate constraint". The case without heating rate constraint has hasty variations in the most states as well as altitude and short final time. However, in an angle of attack, the case with heating rate constraint has a many hasty variations since the heating rate constraint should be satisfied. Although the case with heating rate constraint does not approach to zero exactly, the results of the Hamiltonian gives strong evidence that the trajectories obtained via global orthogonal polynomial is close to optimal trajectories.

Acknowledgements

This work was supported by the Korea Research Foundation Grant funded by the Korean Government (MOEHRD) (KRF-2005-003-D00059).

References

B. P. and Sng, K. B., 1980, "Numerical Solution of the Constrained Re-Entry Vehicle Trajectory Problem via Quasilinearization," *Journal of Guidance, Control, and Dynamics*, Vol. 3, No. 5, pp. 392~397.

Baker, C. D., Causey, W. E. and Ingram, H. L., 1971, "Mathematical Concepts and Historical Development of the MOSCOT Guidance Technique for Space Vehicle," *NASA Technical Memorandum*, NASA TM-44408.

Betts, J. T., 2001, *Practical Methods for Optimal Control Using Nonlinear Programming*, SIAM : Advances in Control and Design Series, Philadelphia, PA.

Betts, J. T., 1998, "Survey of Numerical Methods for Trajectory Optimization," *Journal of Guidance, Control, and Dynamics*, Vol. 21, No. 2, pp. 193~207.

Bryson, A. E. and Ho, Y. C., 1975, *Applied Optimal Control*, Hemisphere Publishing Corporation, WA.

Bryson, A. E., 1999, *Dynamic Optimization*, Addition Wesley, Longman, Menlo Park, CA.

Calise, A. J. and Leung, S. K., 1994, "Hybrid Approach the Solution of Optimal Control Problem," *Journal of Guidance, Control, and Dynamics*, Vol. 17, No. 75, pp. 966~974.

Elnagar, G. N. and Razzaghi, M., 1997, "A Collocation-Type Method For Linear Quadratic Optimal Control Problem," *Optimal Control Application and Methods*, Vol. 18, pp.227~235.

Fahroo, F. and Ross, I. M., 1998, "Costate Estimation by a Legendre Pseudospectral Method," *Journal of Guidance, Control, and Dynamics*,

Vol. 24, No. 2, pp. 270~277.

Han, B. K., Chung, K. and Han, D. S., 1989, "Vibration Analysis on Plates By Orthogonal Polynomial," *KSME International Journal*, Vol. 3, No. 2, pp. 95~102.

Hull, D. G., 1997, "Conversion of Optimal Control Problem into Parameter Optimization Problems," *Journal of Guidance, Control, and Dynamics*, Vol. 20, No. 1, pp. 57~60.

Jinhee Lee, 2003a, "In-Plane Free Vibration Analysis of Curved Timoshenko Beams by the Pseudospectral Method," *KSME International Journal in Korea*, Vol. 17, No. 8, pp.1156~1163.

Jinhee Lee, 2003b, "Application of the Chebyshev-Fourier Pseudospectral Method to the Eigenvalue Analysis of Circular Mindlin Plates with Free Boundary Conditions," *KSME International Journal* in Korea, Vol. 17, No. 10, pp. 1458~1465.

Lee, D. W. and Cho, K. R., 2000, "Flight Range Control of Atmosphere Re-Entry Vehicle Using the Reference Trajectory Correction," *Journal of The Korean Society for Aeronautical and Space Sciences*, Vol. 28, No. 6, pp. 77~85.

Lee, D. W. and Cho, K. R., 2002, "Reference Trajectory Analysis and Trajectory Control by the Bank Angle for Re-Entry Vehicle," *KSME International Journal*, Vol. 16, No. 6, pp. 745~756.

Lee, D. W. and Cho, K. R., 2004, "Re-Entry Trajectory Tracking Via an Inverse Dynamics Methods," *KSME International Journal*, Vol. 18, No. 9, pp. 1519~1528.

Lu, P., 1997, "Entry Guidance and Trajectory Control for Reusable Launch Vehicle," *Journal of Guidance, Control, and Dynamics*, Vol. 20, No. 1, pp. 143~149.

Regan, F. J., 1993, *Dynamics of Atmospheric Re-Entry*, AIAA Education Series.

Vinh, N. X., Busemann, A. and Culp, R. D. 1980, *Hypersonic and Planetary Entry Flight Mechanics*, Univ. of Michigan Press, Ann Arbor, MI.